InN/InGaN multiple quantum wells emitting at 1.5 μm grown by molecular beam epitaxy

J. Grandal,[1,a)] J. Pereiro,[1,b)] A. Bengoechea-Encabo,[1] S. Fernández-Garrido,[1,c)] M. A. Sánchez-García,[1] E. Muñoz,[1] E. Calleja,[1] E. Luna,[2] and A. Trampert[2]
[1]*Departamento de Ingeniería Electrónica and ISOM, ETSI Telecomunicación, Univ. Politécnica de Madrid, Ciudad Universitaria, s/n, 28040-Madrid, Spain*
[2]*Paul-Drude-Institut für Festkörperelektronik, Hausvogteiplatz 5-7, 10117 Berlin, Germany*

(Received 19 November 2010; accepted 12 January 2011; published online 7 February 2011)

This work reports on the growth by molecular beam epitaxy and characterization of InN/InGaN multiple quantum wells (MQWs) emitting at 1.5 μm. X-ray diffraction (XRD) spectra show satellite peaks up to the second order. Estimated values of well (3 nm) and barrier (9 nm) thicknesses were derived from transmission electron microscopy and the fit between experimental data and simulated XRD spectra. Transmission electron microscopy and XRD simulations also confirmed that the InGaN barriers are relaxed with respect to the GaN template, while the InN MQWs grew under biaxial compression on the InGaN barriers. Low temperature (14 K) photoluminescence measurements reveal an emission from the InN MQWs at 1.5 μm. Measurements as a function of temperature indicate the existence of localized states, probably due to InN quantum wells' thickness fluctuations as observed by transmission electron microscopy. © *2011 American Institute of Physics*. [doi:10.1063/1.3552195]

The InN band gap value (~0.7 eV) and the predicted high electron mobility (~14 000 $cm^2/V\,s$) significantly enhance the interest on InN-based heterostructures for photovoltaic devices (multijunction solar cells) and high power/high speed electronic devices.[1,2] InN-based alloys are also promising materials for high-efficiency optoelectronic devices (laser diodes and detectors) for optical communications in the near infrared (IR) range. Most efforts currently aim to achieve p-type InN layers[3] as well as to grow high quality multiple quantum wells (MQWs) heterostructures,[4–7] being that both issues are essential to fabricate efficient devices. Conventional IR optoelectronic devices based on In(Ga)N require a p-type layer on top of a MQWs structure, but Mg-doping of In-rich InGaN layers is still a challenge because of the intrinsic high n-type conductivity and surface electron accumulation in InN.

This work focuses on the structural and optical characterization of InN/InGaN MQWs grown by plasma assisted molecular beam epitaxy on commercial GaN templates (Lumilog) with a threading dislocation density (TDD) of 8×10^8 cm^{-2}. Active nitrogen was supplied by a radio frequency plasma source (Addon PRF-N-600), while standard Knudsen effusion cells provided In and Ga. *In situ* growth monitoring was performed by reflection high energy electron diffraction. The MQWs were structurally characterized by transmission electron microscopy (TEM) in a JEOL JEM-3010 microscope and by x-ray diffraction (XRD) using a PANalytical X'pert Pro MRD system. Photoluminescence (PL) was excited by a 780 nm laser diode at 200 mW cm^{-2} and detected with a Hamamatsu P4638 PbS photodetector using lock-in techniques.

After growing a 100 nm thick GaN buffer layer at 700 °C under Ga-stable conditions,[8] the substrate temperature was decreased down to 475 °C to grow the InN/InGaN MQWs structures with five and ten QWs and a nominal 15% Ga composition in the barriers. In order to avoid surface roughness and to minimize the InN decomposition, the InN QWs and the InGaN barriers were grown under metal rich conditions without interruptions, i.e., both the InGaN barriers and the InN wells were grown at the same temperature. The *ex situ* analysis performed by TEM indicates no In clustering throughout the whole structure even though the surface was

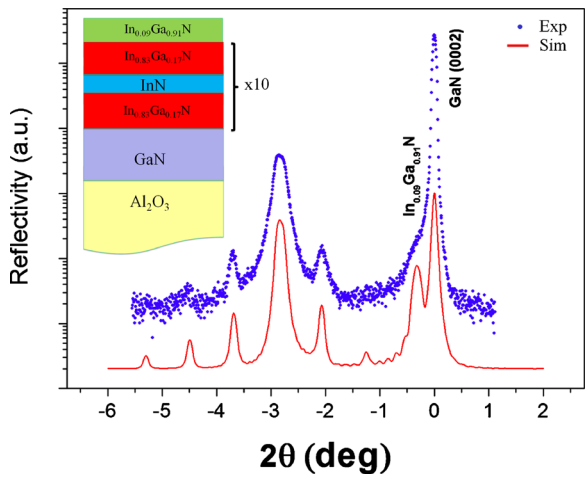

FIG. 1. (Color online) XRD scan and simulation of one sample with 10 × InN quantum wells; satellite peaks up to the second order are observed. The estimated Ga composition in the barriers is 17%. The well and barrier thicknesses are 3.0 and 9.0 nm, respectively. A low temperature (500 °C) $In_{0.09}Ga_{0.91}N$ cap layer was grown on top. The inset shows the scheme and nominal parameters of the samples grown.

[a)]Present address: Department of Electrical and Computer Engineering, The Ohio State University, 205 Dresse Laboratory, 2015 Neil Avenue, Columbus, Ohio 43210, USA. Electronic mail: jgrandal@die.upm.es.
[b)]Present addresses: School of Physical and Mathematical Sciences, Division of Physics and Applied Physics, Nanyang Technological University, 21 Nanyang Link, Singapore 637371 and Department of Condensed Matter Physics and Material science, Brookhaven National Laboratory, Upton, 11973 New York, USA.
[c)]Present address: Paul-Drude-Institut für Festkörperelektronik, Hausvogteiplatz 5-7, 10117 Berlin, Germany.

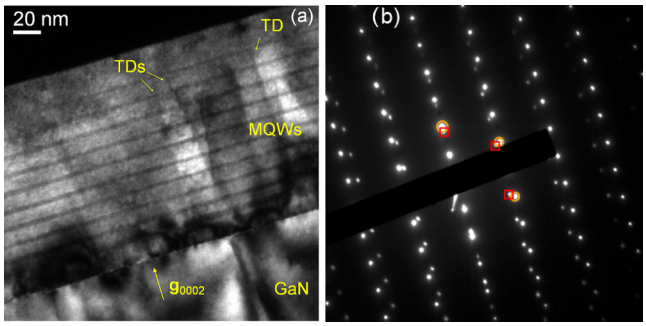

FIG. 2. (Color online) (a) Cross-sectional dark-field TEM image of the 10 $\times$InN/$In_{0.83}Ga_{0.17}N$ heterostructure (TD: threading dislocations). (b) SAED image revealing two different diffraction patterns: (circles) GaN and (squares) relaxed InGaN barriers and the compressively strained InN QWs.

covered by In droplets as observed using an optical microscope. This indicates that the metal excess was accumulated on top of each layer.

Finally, on top of the last InGaN barrier, a 90 nm thick capping layer of InGaN, with a nominal In composition of 10%, was grown at 500 °C. All attempts of growing a high temperature GaN or Ga-rich InGaN cap layer at higher temperature led to the full decomposition of the QWs.

XRD scans from the MQWs show satellite peaks up to the second order independently of the number of QWs. This feature is typical for heterostructures with abrupt interfaces (Fig. 1) and confirms the presence of the QWs. In order to estimate the barrier composition and the wells and the barriers thicknesses, XRD simulations were performed. The results agree well with nominal growth parameters, yielding an estimated 17% Ga barrier composition. The thicknesses of the well/barrier were estimated to be 3.0 nm/9.0 nm, respectively (Fig. 1). The best fit is obtained assuming fully relaxed barriers with respect to the GaN template and fully compressed wells with respect to the barriers. The In composition estimated for the capping layer by XRD simulations is 9%. The measurements performed by TEM confirmed these results and assumptions. Figure 2(a) shows a cross-sectional dark-field TEM image along the $\langle 11-20\rangle$ zone axis of a 10 $\times$(InN/InGaN) MQWs sample using the diffraction vector $\mathbf{g}=0002$. At first sight, QWs and barriers follow a periodic sequence with well defined interfaces. The measured average thicknesses of the QWs and barrier layers, obtained from the dark-field images, are in good agreement with the values inferred from XRD. A careful inspection, however, reveals remarkable thickness fluctuations (± 1 nm) on the nanometer scale, which are additionally affected by the presence of threading dislocations (marked in the micrograph) passing the whole MQWs structure. The TDD for the InN QWs layer is estimated to be about 4×10^{10} cm^{-2}. Selected area electron diffraction (SAED) pattern reveals the presence of two sets of spots [Fig. 2(b)]: one set associated with the GaN template (circles) and another one related to the relaxed InGaN barriers and the strained InN wells (squares).

Low temperature (14 K) PL spectra show two emission peaks for all samples: a well resolved one at 1.5 μm and a second one at 1.6 μm, as determined from two Gaussian curve fittings [Fig. 3(a)].

Theoretical predictions (finite element Schrödinger–Poisson calculations) using the physical parameters for InGaN and InN taken from Wu and Walukiewicz[9] suggest that the emission at 1.5 μm is associated to a band to band transition within the QW. On the other hand, the peak at 1.6 μm could be attributed to transitions from deep acceptors generated by structural defects within the crystal, as reported in InN layers by several groups.[10,11] Miller *et al.*[12] suggested that the origin of this peak could be related with unintentional contamination from a hydrogenic acceptor. They estimated the energy of a hydrogenic acceptor assuming the hole effective mass to fall in the range $m^*_h=0.42-0.7m_o$ and using $\varepsilon_o=10.3$ as the static dielectric constant.[13] The acceptor ionization energy is estimated to be in the range of 54–90 meV, which is consistent with the peak we obtain at 1.6 μm. However, the origin of these deep acceptor states still remain unclear and further analysis should be performed. In order to ascertain the origin of these two emissions, peak energy and integrated intensity temperature dependence were investigated. From the PL spectra evolution with temperature in Fig. 3(a), the energy dependence for the two peaks is plotted in Fig. 3(b), showing very different behaviors. While the emission at 1.5 μm shows a clear S-shape behavior [Fig. 4(a)], the one at 1.6 μm has no clear dependence (not shown). In the first case, the energy decreases (redshift) in the range of 14–95 K, then increases (blueshift) from 95 to 215 K, and finally decreases again (redshift) for temperatures above 250 K. This S-shape behavior has been generally attributed to carrier localization.[14–16] A fitting of the evolution of the integrated intensity as a function of the temperature could determine the characteristic activation energy of the process or processes involved in the thermal quenching of the emission from the wells. The expression used to estimate the activation energy is[17]

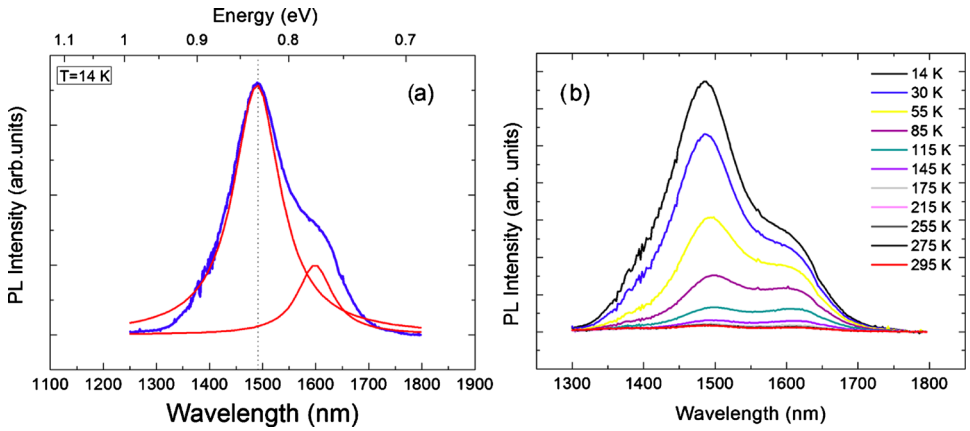

FIG. 3. (Color online) (a) PL spectrum of 5 $\times$InN/$In_{0.83}Ga_{0.17}N$ at low temperature (14 K). Two luminescence peaks are observed coming from the InN wells. (b) PL spectra of 5 $\times$InN/$In_{0.83}Ga_{0.17}N$ as a function of temperature.

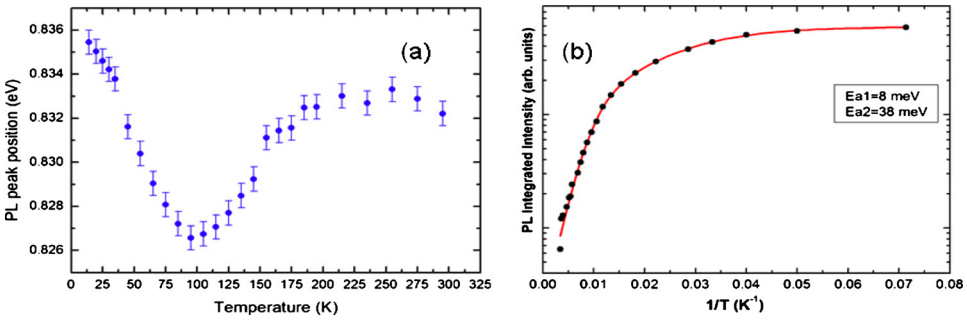

FIG. 4. (Color online) (a) PL main peak position as a function of temperature of a $5\times InN/In_{0.83}Ga_{0.17}N$ sample. (b) Arrhenius plot of the integrated intensity.

$$I(T) = \frac{I(0)}{1 + C \cdot \exp\left(\frac{-E_{act}}{K_B T}\right)},$$

where $I(0)$ is the integrated intensity of the emission at 0 K, E_{act} is the activation energy, k_B is the Boltzmann's constant, and C is a fitting constant. However, if we consider just one activation energy, the experimental data do not fit properly, which indicates that more than one process may be involved in the PL quenching.

Though theoretically, several processes may be involved in the PL quenching; when considering two processes, the equation above can be written as follows:[17]

$$I(T) = \frac{I(0)}{1 + C_1 \cdot \exp\left(\frac{-E_{1,act}}{K_B T}\right) + C_2 \cdot \exp\left(\frac{-E_{2,act}}{K_B T}\right)},$$

where $I(0)$ is the integrated intensity of the emission at 0 K and $E_{1,act}$ and $E_{2,act}$ are the activation energies of the processes related with the thermal quenching. Figure 4(b) shows the fit of the integrated intensity where the best fit is obtained assuming two processes with activation energies of 8 and 38 meV, respectively. Grenouillet *et al.*[16] suggested that the PL intensity quenching between 8 and 100 K is typical of strong localization effects in InGaN QWs. In this sense, we may attribute the smaller activation energy to delocalization of carriers and the larger one to the quenching of luminescence from thermal activation of defects.[17]

Retrieving the results from TEM, we tentatively explain this localization phenomenon considering the confinement energy fluctuations caused by the observed thickness variations within the QWs. However, further studies, out of the scope of this work, are needed to discard other possible explanations such as defect-induced inhomogeneous strain distribution within the QWs.

In conclusion, high quality InN/InGaN MQWs were grown by molecular beam epitaxy with a PL emission at 1.5 μm. The PL peak position as a function of the temperature presented a characteristic S-shape (decrease-increase-decrease), attributed to carrier localization effects. TEM observations together with the calculations on the PL emission indicate that the localized states are probably due to thickness fluctuations of the InN quantum wells. The InGaN barriers are relaxed with respect to the GaN substrate, while the InN QWs grow compressively strained on the InGaN barriers, as confirmed by both TEM and XRD results.

The authors would like to thank Ž. Gačević and Dr. P. Lefevbre for fruitful discussions about the optical characterization and Dr. L. Cerutti for providing the Schrödinger solver. Thanks are also due to H. v. Kiedrowski and A. Pfeiffer for their assistance with the TEM sample preparation. The authors wish also to acknowledge partial support by the Spanish Ministry of Education and Science, Project Nos. MAT2008-04815, "Strategic Japanese-Spanish Cooperative Program" MICINN PLE2009-0023, and Consolider CSD2006-00019 and by the CAM Project (IV PRICYT) Grant No. S-0505/ESP-0200.

[1] V. Yu. Davydov, A. A. Klochikhin, R. P. Seisyan, V. V. Emtsev, S. V. Ivanov, F. Bechstedt, J. Furthmüller, H. Harima, A. V. Mudryi, J. Aderhold, O. Semchinova, and J. Graul, Phys. Status Solidi B **229**, r1 (2002).
[2] V. M. Polyakov and F. Schwierz, Appl. Phys. Lett. **88**, 032101 (2006).
[3] R. E. Jones, K. M. Yu, S. X. Li, W. Walukiewicz, J. W. Ager, E. E. Haller, H. Lu, and W. J. Schaff, Phys. Rev. Lett. **96**, 125505 (2006).
[4] S. B. Che, W. Terashima, Y. Ishitani, A. Yoshikawa, T. Matsuda, H. Ishii, and S. Yoshida, Appl. Phys. Lett. **86**, 261903 (2005).
[5] A. Yoshikawa, S. B. Che, W. Yamaguchi, H. Saito, X. Q. Wang, Y. Ishitani, and E. S. Hwang, Appl. Phys. Lett. **90**, 073101 (2007).
[6] M. Kurouchi, H. Na, H. Naoi, D. Muto, S. Takado, T. Araki, T. Miyajima, and Y. Nanishi, Phys. Status Solidi C **3**, 1599 (2006).
[7] S. Hirano, T. Inoue, G. Shikata, M. Orihara, Y. Hijikata, H. Yaguchi, and S. Yoshida, J. Cryst. Growth **301–302**, 513 (2007).
[8] G. Koblmüller, S. Fernández-Garrido, E. Calleja, and J. S. Speck, Appl. Phys. Lett. **91**, 161904 (2007).
[9] J. Wu and W. Walukiewicz, Superlattices Microstruct. **34**, 63 (2003).
[10] A. A. Klochikhin, V. Yu. Davydov, V. V. Emtsev, A. V. Sakharov, V. A. Kapitonov, B. A. Andreev, H. Lu, and W. J. Schaff, Phys. Rev. B **71**, 195207 (2005).
[11] B. Arnaudov, T. Paskova, P. P. Paskov, B. Magnusson, E. Valcheva, B. Monemar, H. Lu, W. J. Schaff, H. Amano, and I. Akasaki, Phys. Rev. B **69**, 115216 (2004).
[12] N. Miller, J. W. Ager III, H. M. Smith III, M. A. Mayer, K. M. Yu, E. E. Haller, W. Walukiewicz, W. J. Schaff, C. Gallinat, G. Koblmüller, and J. S. Speck, J. Appl. Phys. **107**, 113712 (2010).
[13] T. Inushima, K. Fukui, H. Lu, and W. J. Schaff, Appl. Phys. Lett. **92**, 171905 (2008).
[14] Y. Cho, G. Gainer, A. Fischer, J. Song, S. Keller, U. Mishra, and S. DenBaars, Appl. Phys. Lett. **73**, 1370 (1998).
[15] K. Ramaiah, Y. Su, S. Chang, B. Kerr, H. Liu, and I. Chen, Appl. Phys. Lett. **84**, 3307 (2004).
[16] L. Grenouillet, C. Bru-Chevallier, G. Guillot, P. Gilet, P. Duvaut, C. Vannuffel, A. Million, and A. Chenevas-Paule, Appl. Phys. Lett. **76**, 2241 (2000).
[17] E. Monroy, N. Gogneau, F. Enjalbert, F. Fossard, D. Jalabert, E. Bellet-Amalric, L. Si Dang, and B. Daudin, J. Appl. Phys. **94**, 3121 (2003).